

# Studies on the Structure of Activated Carbon Fibers Activated by Phosphoric Acid

Ruowen Fu,<sup>1</sup> Ling Liu,<sup>1</sup> Wenqiang Huang,<sup>2</sup> Pingchun Sun<sup>2</sup>

<sup>1</sup>Materials Science Institute, PCFM Laboratory, Zhongshan University, Guangzhou, China

<sup>2</sup>State Key Laboratory of FPMAS, Nankai University, Tianjin, China

Received 31 October 2001; accepted 14 May 2002

**ABSTRACT:** By solid-state <sup>13</sup>C- and <sup>31</sup>P-NMR, XPS, and FTIR, the chemical structure of activated carbon fiber–P (ACF-P) and its reaction with phosphoric acid were studied. Even when activated at low temperatures, these fibers developed a graphitelike carbon structure with a certain amount of phenol groups as well as acetal (or methylenedioxy) carbon. As expected, the oxygen-containing groups were greatly reduced at high activation temperatures. Different from the ACF-W, metaphosphoric acid (or polyphosphates) and a small amount of phosphorus exist on ACF-P. The original ACF-P activated at low temperature contained a lot of phosphoric acid, so it had to be

washed with water to expose the large surface area. The washing process can be omitted for ACF-P activated at high temperature because most phosphorus compounds in fiber have volatilized. The ACF-P activated at lower temperature possessed a large amount of oxygen-containing surface groups and had enhanced adsorption ability for polar adsorbates. The remaining of metaphosphoric acid enhanced the adsorption of silver ion. The experimental results showed that the peaks of <sup>31</sup>P-NMR, P<sub>2p</sub>-XPS, and FTIR at 1620 cm<sup>-1</sup> shifted with the increase of activated temperature. © 2003 Wiley Periodicals, Inc. *J Appl Polym Sci* 87: 2253–2261, 2003

## INTRODUCTION

It is well known that activated carbon fibers (ACFs) are one kind of highly effective fibrous adsorbent with high specific surface area, abundant micropores, small diameter, minimized external, and intradiffusional resistance to mass transfer, thereby exhibiting high adsorption capacity and velocity. Nowadays, ACFs have been successfully applied in many fields, such as the treatment of organic and inorganic waste gases, the recovery of organic solvent, air cleaning and deodorization, treatment of wastewater and drinking water, separation and recovery of precious metals, as medical adsorbents and protective articles, and in electrodes.<sup>1–3</sup> To reduce production costs, in our previous work,<sup>4–7</sup> we prepared a new kind of ACF (ACF-P) from sisal fiber (low-cost precursor) by phosphoric acid activation at low temperature (low energy consumption). The results showed that ACF-P possesses high yield (30–40 wt %), large surface area (900–950 m<sup>2</sup>/g), and

high static adsorption capacities and good dynamic adsorbability for organic vapors.

In the last decades some scientists have paid attention to the structural studies of ACFs and to exploring the relationship between structure and properties. Tang and Bacon investigated the pyrolysis of cellulose and summarized its carbonization mechanism.<sup>8</sup> Mangun et al. studied the structures and properties of oxidized ACFs by means of DRIFTS and X-ray photoelectron spectroscopy (XPS) and concluded that oxidation produces surface chemistries in the pores of fibers, providing for enhanced adsorption of basic and polar molecules.<sup>9</sup> Shin et al. studied the effect of heat treatment on functional groups of pitch-based ACF using Fourier transform infrared spectroscopy (FTIR) and confirmed that as the heat-treatment temperature increased, the amount of oxygen-containing surface functional groups was reduced and the ACFs became more hydrophobic.<sup>10</sup> Kaneko et al. systematically investigated the pore structures of ACFs.<sup>11,12</sup> In addition, some studies on the structural surface of carbon fibers and activated carbons by XPS and <sup>13</sup>C-NMR can also be found in the literature.<sup>13–19</sup> In our previous studies, we also made efforts to understand the structure of ACFs using various modern analytic techniques and obtained some interesting results.<sup>20–22</sup> Unfortunately, there is very little in the literature, if any,

Correspondence to: R. Fu (cesfrw@zsunlink.zsu.edu.cn).

Contract grant sponsors: Major Natural Science Foundation of Guangdong Province; Team Project of Guangdong Province; Foundation for the Key Teachers in China University.

related to the chemical structure and activation mechanism of sisal-based ACF-P activated with phosphoric acid.

Compared with coals, wood, cotton stalks, wheat, and coconut shell, which have been reported to be activated to produce granular carbons,<sup>23-27</sup> sisal fiber possesses a distinctive chemical and textural structure.<sup>28</sup> It is a natural polymer, mainly composed of cellulose, hemicellulose, and lignin. It has high crystallinity and the (002) planes of a sisal crystalline lattice are preferentially oriented at an angle of  $10.6^\circ$  to the axis with an orientation extent of 85.5%. To provide some new ideas for controlling the preparation of ACF-P or to design new kinds of chemically activated porous carbons, it was necessary to further investigate the chemical change and activation mechanism of sisal fiber activated with phosphoric acid. Therefore, the objectives of the present research were to explore: (a)

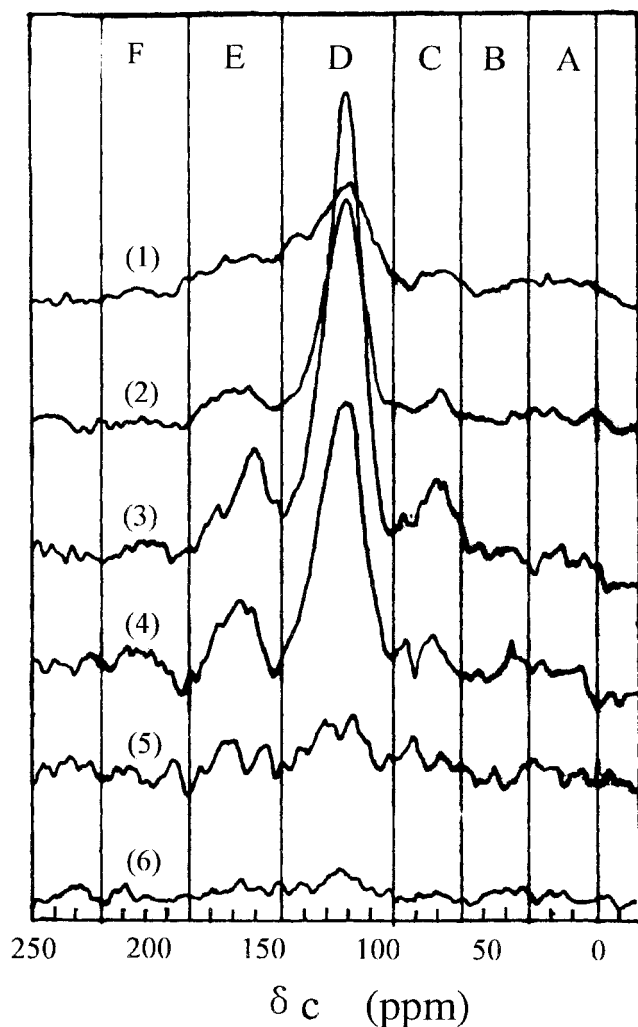


**Figure 1**  $^{13}\text{C}$ -NMR spectra of ACF-P-xxx-1 activated at different temperatures: (1) 250°C, (2) 350°C, (3) 400°C, (4) 500°C, (5) 750°C, (6) 830°C.

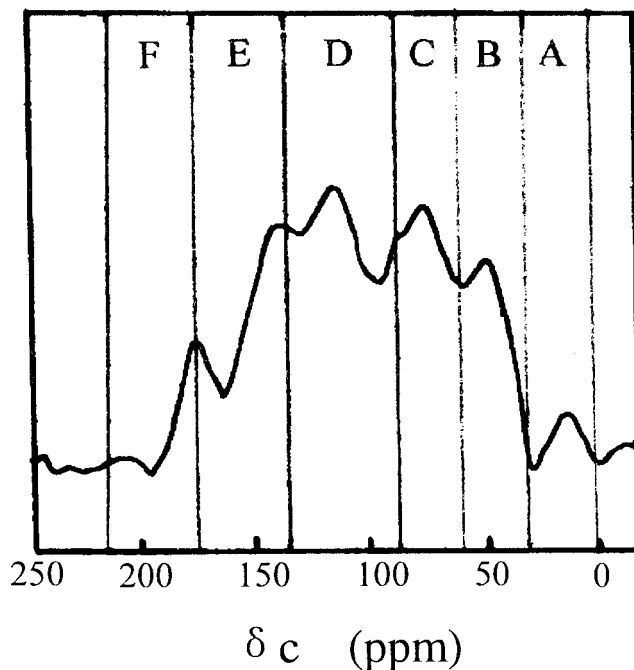


**Figure 2**  $^{13}\text{C}$ -NMR spectrum of PVFACF activated at 700°C.

the chemical structure (including matrix carbon structure and surface groups) of ACF-P produced; (b) the reactions of phosphoric acid during activation; and (c) the effects of chemical structures derived from different activation processes or conditions on the adsorption properties of the ACF-P.

## EXPERIMENTAL

### Preparation of ACF-P

About 40 g of natural sisal fiber was immersed with 35% of  $\text{H}_3\text{PO}_4$  for 24 h and then taken out from solution and dried. The treated fiber was hung in a carbonization-activation furnace, heated to a predetermined temperature and kept at this temperature for 90 min in the protection of nitrogen gas. After cooling to ambient temperature, the product was removed and denoted as ACF-P-xxx-0. Here, xxx represents the activation temperature. When ACF-P-xxx-0 was fully washed with water and then dried, the obtained fiber was denoted as ACF-P-xxx-1.

The physically activated sample (denoted as ACF-W) was made by hanging about 40 g of natural sisal fiber impregnated with 5%  $(\text{NH}_4)_2\text{HPO}_4$  in a carbonization-activation furnace. The sample was heated to 830°C and kept at this temperature for 30 min. Then it was activated with steam at this temperature for 90 min in the protection of nitrogen gas.

TABLE I  
Relationship Between Activation Temperature and Surface Area and Adsorption Properties of ACF-P-xxx-1

Activation temperature (°C)	250	300	350	500	750	830
Surface area (m <sup>2</sup> /g)	267	740	938	615	822	960
Adsorption capacity of carbon tetrachloride (mmol/g)	/	5.34	7.41	4.19	4.26	5.25
Adsorption capacity of benzene (mmol/g)	2.11	4.02	5.85	5.14	4.56	4.65
Adsorption capacity of methanol (mmol/g)	5.38	11.68	15.12	13.06	8.75	9.0

### Characterization of ACF-P

The fibers were ground into powder and packed into sample tubes. Solid-state <sup>13</sup>C-NMR spectra were recorded with a Varian NMR spectrometer (Varian, Palo Alto, CA) using the CPMAS technique (hexamethylbenzene as standard; in this study the  $\delta_c$  was 17.3 ppm smaller than that detected by using tetramethylsilane as standard). The <sup>31</sup>P-NMR spectra were recorded directly (NaH<sub>2</sub>PO<sub>4</sub> as standard).

The X-ray photoelectron spectra were recorded with a Vacuum Generator Escalab MK II spectrometer (VG Scientific, East Grinstead, UK) using Mg K $\alpha$ X radia-

tion at 240 W (12 kV). Calibration was done by assuming a binding energy (BE) of C<sub>1s</sub> of the contaminating carbon equal to 284.3 eV. Data analysis (smoothing, deconvolution, curve fitting, X-ray satellite subtraction, background subtraction, normalization, etc.) was done by a microcomputer. The specimens were fixed to a sample holder with double-sided adhesive tape. The vacuum system was kept at about  $1 \times 10^{-6}$  Pa.

Specimens were ground with KBr and pressed into disks. They were then analyzed by a model 205 Nicolet FTIR spectrometer (Nicolet, Madison, WI). The samples were ground to a powder and pressed into sample holders. The powder X-ray diffraction patterns were obtained using a Rigaku model D/max III A X-ray diffractometer (Rigaku, Tokyo, Japan). The BET surface areas of ACF-P were measured by a model ST-03 surface and pore distribution detector.

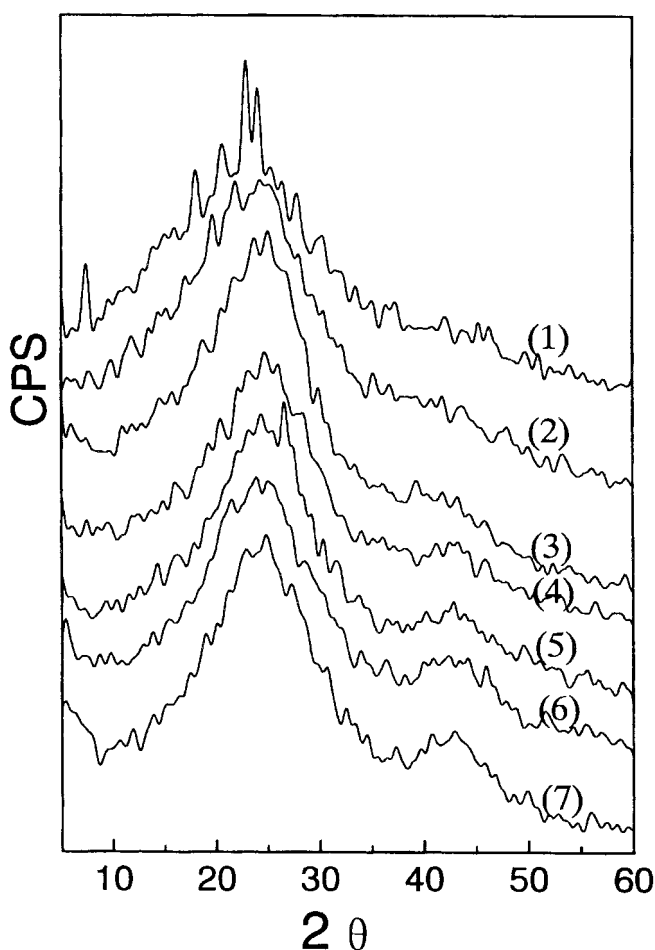


Figure 3 XRD pattern of ACF-P-xxx-1 activated at different temperatures: (1) 250°C, (2) 300°C, (3) 350°C, (4) 400°C, (5) 500°C, (6) 750°C, (7) 830°C.

### Adsorption experiments

The adsorption capacities of saturated organic vapors at 30°C were measured by gravimetric analysis described in detail previously.<sup>6</sup>

The adsorption of silver was carried out by soaking a certain amount of ACF-P in 0.02M AgNO<sub>3</sub> solution at 30°C for 24 h and then separating the fiber from the solution with filter paper. The adsorption capacity of ACF-P for silver was calculated from the difference of silver concentrations before and after adsorption,

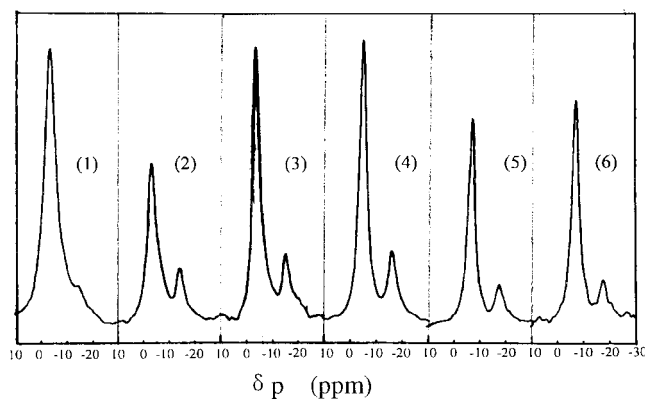
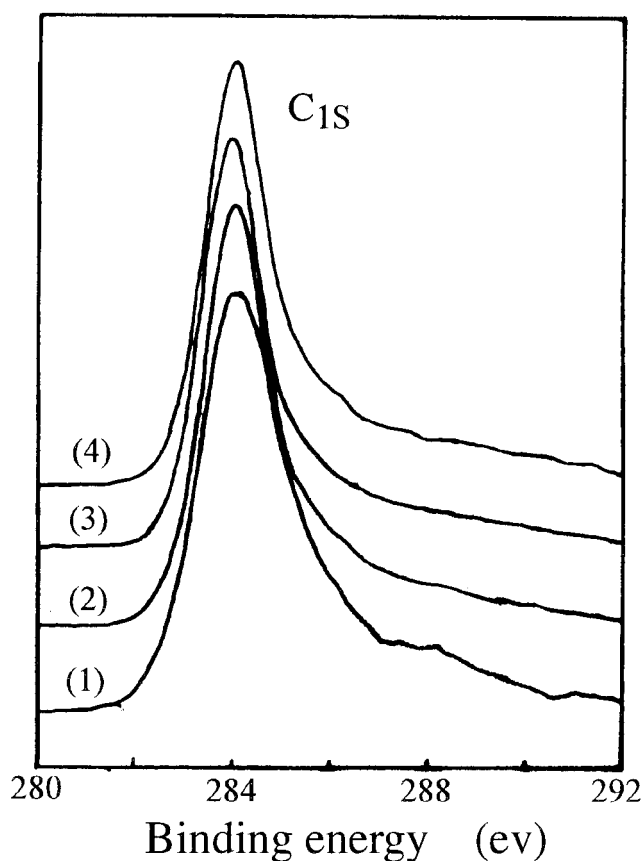


Figure 4 <sup>31</sup>P-NMR spectra of ACF-P-xxx-1 activated at different temperatures: (1) 250°C, (2) 350°C, (3) 400°C, (4) 500°C, (5) 750°C, (6) 830°C.



**Figure 5** XPS  $C_{1s}$  spectra of ACF-P-xxx-1 activated at different temperatures: (1) 250°C, (2) 350°C, (3) 500°C, (4) 830°C.

which was determined by a WFX-1C atomic adsorption spectrometer made in China.

## RESULTS AND DISCUSSION

### $^{13}C$ -NMR spectra of ACF-P

Figure 1 shows the  $^{13}C$ -NMR spectra of the ACF-P prepared at different temperatures. We divide the resonance spectra into six bands denoted from A to F. According to the literature,<sup>19,22,29–31</sup> the assignment of all the resonance peaks (A, B, D, E, and F), except for C, is undoubted. It is commonly concluded that the peak at 10–20 ppm in band A is assigned to methyl and methylene groups. The peak at 40–45 ppm in band B is assigned to the structures of  $-C-O-$ , which include  $-C-OH$  and  $-C-O-C-$ . The peak

at 100–130 ppm in band D is the typical chemical shift of aromatic carbon structure. The peaks in band E and F are assigned to phenol and carbonyl groups, respectively.

It can be seen from Figure 1 that there is a distinguished peak in band C, which had a high intensity when the activation temperature was below 500°C. According to the literature,<sup>32,33</sup> a resonance having a chemical shift around 80 ppm may be caused by alkynyl carbon or acetal (or methylenedioxy) carbon. According to the FTIR results of our earlier study<sup>21</sup> and Figure 9 in the latter of this paper, no characteristic IR peak of alkynyl group can be seen. The IR peak appearing at 1000–1200  $cm^{-1}$  corresponds to the acetal (or methylenedioxy) group. Therefore, we propose that the peak in band C be assigned to acetal (or methylenedioxy) carbon. A further reviewing of the  $^{13}C$  spectrum of PVFACF in the literature<sup>22</sup> (and its second figure) (see Fig. 2) indicates the peak at 80 ppm also suggests the existence of acetal (or methylenedioxy) carbon because the PVFACF was made from poly(vinyl formaldehyde) fiber, which originally contains a large amount of acetal carbon.

According to the changes of peak intensity in Figure 1, the chemical changes and relative structure of ACF-P are the following:

1. When activation temperature rose to 350°C, the resonance intensity of aromatic carbon in band D increased obviously. X-ray diffraction (XRD) analysis (Fig. 3) also shows that graphitelike structure starts to form at about this temperature. There is a synchronous increase of adsorption ability with the formation of graphitelike aromatic structure. Table I shows that the surface area and adsorption ability of ACF-P are at a maximum when activation temperature is 350°C. The previous study<sup>7</sup> showed that ACF-P activated below 300°C had very poor dynamic adsorption ability for benzene, whereas that prepared above 350°C possessed strong dynamic adsorption ability. So we conclude that the formation of graphitelike aromatic structure plays a role in the enhancement of adsorption ability of ACF-P. If the activation temperature is held below 300°C, many carbon atoms may still be in the  $SP^3$  state, so the fibers obtained possess weak adsorption affinity for the adsorbate.

**TABLE II**  
Chemical Shift of Two  $^{31}P$ -NMR Peaks of the ACF-P-xxx-1 Activated at Different Activation Temperatures

Activation temperature (°C)	250	300	350	500	750	830
Shift of peak 1	-3.379	-3.620	-4.103	-5.068	-6.516	-6.999
Shift of peak 2	/	-14.480	-14.936	-16.170	-17.135	-17.377

TABLE III  
XRD Parameters of ACF-P-xxx-1

Activation temperature (°C)	300	350	400	500	750	830
$d_{002}$ (nm)	0.3863	0.3767	0.3751	0.3735	0.3705	0.3705
Lc (nm)	0.728	0.861	0.902	0.911	0.929	0.948
La (nm)	/	1.998	2.220	2.350	2.497	2.854

- It was found that the intensity of the phenol peak in band E and the acetal peak in band C increased with increasing activation temperature at first and then decreased after 500°C and 400°C, respectively. In previous studies<sup>10,21</sup> it was also observed that the amount of oxygen-containing groups would be reduced as heat treatment temperature increased.
- The peaks in bands A, B, and F, shown in Figure 1, were always weak, no matter the activation temperature, suggesting the amounts of methyl, methylene, and carbonyl groups in ACF-P, if they existed, were small.
- When the activation temperature was greater than 750°C, the signal of resonance spectra was quite weak because most surface groups were removed and aromatic rings were enlarged into graphitelike microcrystals, with a consequent decrease in hydrogen content, which weakened the cross-polarization of H and C.

### <sup>31</sup>P-NMR spectra of ACF-P

Figure 4 shows the <sup>31</sup>P-NMR spectra of ACF-P activated at different temperatures. The two resonance peaks presented indicate that there were two kinds of phosphorus compounds on ACF-P. This is different from ACF-W, on which only an oxide (mainly phosphorus pentoxide) was formed.<sup>22,34</sup> It is well known that phosphoric acid will be changed into metaphosphoric acid or polyphosphates<sup>23</sup> by heating to a high temperature. Further, compared with the chemical shift of phosphorus compounds on ACF-W<sup>22</sup> and with reference to the P<sub>2p</sub> spectra of XPS, shown in Figure 6 below, the peaks with chemical that shifted from -3.3 to about -7.0 ppm may be assigned to metaphosphoric acid (or polyphosphates). The small peaks with a chemical shift from -14.5 to -17.4 ppm may be assigned to elemental phosphorus because small

amounts of phosphoric acid may be reduced by carbon at high temperature. The existence of phosphorus has also been illustrated by thermogravimetric analysis. When ACF-P was heated in air to 400°C, the weight increased by about 1%, whereas the weight did not change when heated in nitrogen atmosphere. In the same air atmosphere ACF-W would decrease in weight to some extent. The weight increase of ACF-P can be attributed to the oxidation of phosphorus by the hot air to phosphoric oxide.

It is very interesting that when the activation temperature increased, both <sup>31</sup>P-NMR peaks shifted to an increasingly higher magnetic field (Table II). This tendency has also been found in the preparation of ACF-W that was impregnated with diammonium hydrogen phosphate and activated by steam.<sup>22</sup> Although the detailed shift mechanism is unclear now, we propose that the shift may be caused by the interaction of phosphorus with the aromatic carbon ring. There are two possible reasons. One is that the phosphorus compounds in ACF-P may reside on the graphite sheet but not at the edges of graphitelike microcrystal of the fiber, so the positive shielding from the action of  $\pi$  current increases with the enlargement of the aromatic carbon rings. The other possible reason is that the phosphorus atoms are able to receive electrons from aromatic carbon. With the enlargement of the aromatic carbon rings, the electron cloud of phosphorus becomes more dense, and its resonance therefore shifts to a higher magnetic field. The XRD results in Table III confirm that the microcrystallites (graphite sheets) of ACF-P were enlarged with an increase in the carbonization-activation temperature.

### XPS analysis

The elemental contents of various ACF-P were calculated through the XPS determination and are listed in Table IV. A comparison of various washed ACF-Ps

TABLE IV  
Elemental Contents of Various ACF-P as Detected by XPS

Sample	ACF-P-250-1	ACF-P-300-1	ACF-P-500-1	ACF-P-830-1	ACF-P-300-0	ACF-P-830-0
C (at %)	54.14	79.64	77.82	82.85	43.90	82.70
O (at %)	38.06	16.63	16.74	13.46	44.60	13.22
N (at %)	1.40	1.39	1.78	1.28	1.47	0.72
P (at %)	6.41	2.35	3.66	2.41	10.03	3.35

TABLE V  
Surface Areas of Different ACF-Ps

ACF-P	ACF-P-350-0	ACF-P-350-1	ACF-P-400-0	ACF-P-400-1	ACF-P-750-0	ACF-P-750-1	ACF-P-830-0	ACF-P-830-1
Surface area (m <sup>2</sup> /g)	~0	938	~0	600	486	822	911	960

(ACF-P-xxx-1) shows that when the activation temperature increased to 300°C, the carbon content of ACF-P-xxx-1 increased and at the same time the oxygen and phosphorus contents decreased. This suggests that most cellulose units are dehydrated and converted into aromatic carbon. The results of <sup>13</sup>C-NMR and FTIR analysis, shown in Figures 1 and 9, also supported this finding. When the activation temperature rose to 830°C, the noncarbon components were further removed out so that the carbon content increased and oxygen and phosphorus content decreased.

The apparent carbon content of the samples activated at low temperature and not washed with water, such as ACF-P-300-0 was small (Table IV). Their surface area can almost be ignored (Table V). We believe that large amounts of phosphoric acid remain in the fiber pores after activation. After washing with water, phosphoric acid can be dissolved out and micropores are exposed so that the surface area (Table V) and adsorption ability<sup>6,7</sup> of ACF-P obviously increase.

It can be shown with a simple calculation that the dissolved substance is mainly phosphoric acid. Supposing *X* part of phosphorus is washed out, four *X* parts of oxygen will be washed concomitantly if the substances washed are in the form of phosphoric acid radicals. According to the phosphorus contents of ACF-P before and after washing (e.g., the phosphorus contents of ACF-P-300-0 and ACF-P-300-1 were 10.3 and 2.35, respectively), we have

$$(10.3 - X)/(100 - (1 + 4)X) = 2.35/100$$

According to the solution (*X* = 8.70) and Table IV, the calculated elemental contents of this washed sample should be: 77.70% C, 17.34% O, 2.6% N, 2.35% P. These results are close to those of ACF-P-300-1, given in Table IV.

When ACF-P was prepared at high temperature (e.g., 830°C), most of the phosphoric acid volatilized

so that the elemental content of ACF-P remained almost the same before and after washing. The experimental results indicate that the nonwashed ACF-P-830-0 also had a large surface area (Table V) and high adsorption capacity.<sup>6,7</sup> Therefore, the washing process can be omitted if the activation temperature is high enough.

The XPS C<sub>1s</sub> spectra of several ACF-P-xxx-1 are shown in Figure 5. All of them have an asymmetric line shape and broaden on the high-binding energy side, similar to the spectra of ACF-W.<sup>21,34</sup> The growth of peaks at 285.9 and 288.5 eV indicates that there were many phenol groups and a small number of carbonyl (carboxyl) groups on ACF-P. In addition, the content of those oxygen-containing groups increased with the

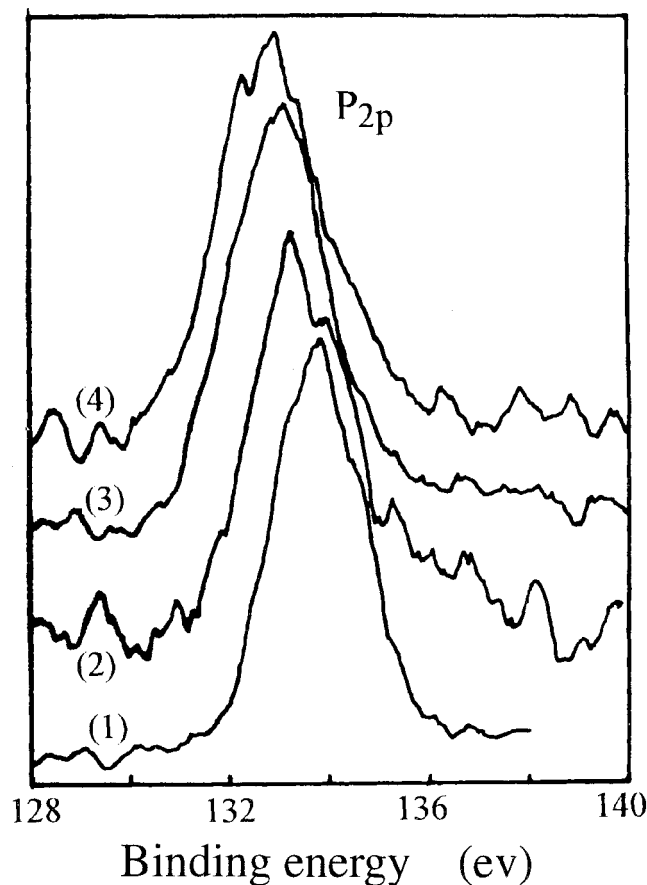


Figure 6 XPS P<sub>2p</sub> spectra of ACF-P-xxx-1 activated at different temperatures: (1) 250°C, (2) 350°C, (3) 500°C, (4) 830°C.

TABLE VI  
Full width at half maximum (FWHM) of C<sub>1s</sub> of ACF-P-xxx-1

ACF-P	ACF-P-250-1	ACF-P-350-1	ACF-P-500-1	ACF-P-830-1
FWHM (eV)	2.19	1.65	1.55	1.53

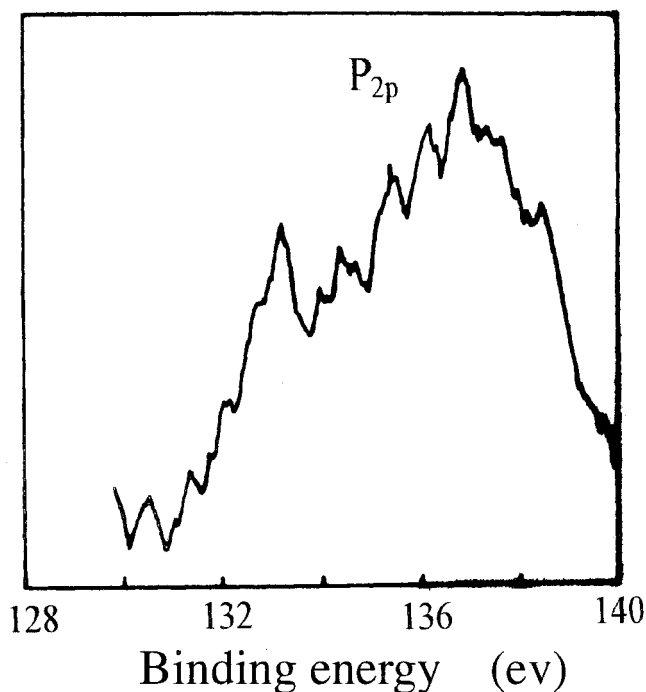


Figure 7 XPS  $P_{2p}$  spectrum of ACF-W impregnated with diammonium hydrogen phosphate.

decrease of activation temperature, judging from the broadening of  $C_{1s}$  FWHM (Table VI) and the increase of the peaks at 285.9 and 288.5 eV. Furthermore, the content of the oxygen-containing group corresponded to the adsorption ability for polar adsorbates. For example, the ACF-P activated at low temperature (350°C) had a higher adsorption capacity for methanol than that activated at high temperature (830°C) because it possessed many more oxygen-containing surface groups. It can also be seen from Table I that the difference of adsorption capacity for polar methanol and nonpolar benzene vapor was enlarged much more for the ACF-P activated at low temperature. Mangun et al. also found that the oxidation of ACF increased the oxygen-containing groups to provide for enhanced adsorption of basic and polar molecules.<sup>9</sup>

The spectral shapes of XPS  $P_{2p}$  of various ACF-P and ACF-W are compared in Figures 6 and 7. The  $P_{2p}$  peaks of ACF-P appearing at 133 to 134 eV may be assigned to metaphosphoric acid (or polyphosphates). Meanwhile, the peak corresponding to phosphorus (at about 130 eV) is too small to be seen. However, the  $P_{2p}$  peak of ACF-W shifted to the high-binding energy side (Fig. 7), which mainly corresponds to a high oxidation state such as phosphorus pentoxide.<sup>35</sup>

It was also observed that the  $P_{2p}$  peak of ACF-P slightly shifted to a lower binding energy when the activation temperature increased (Fig. 6). Two possible reasons may cause this shift. One may be that the phosphorus atom can receive an electron from aromatic carbon, as discussed above.

Another reason may be that the orthophosphoric acid impregnated in the fiber is dehydrated and condensed into pyrophosphoric acid, metaphosphoric acid, and polyphosphates gradually. This hypothesis is also supported by the result shown in Figure 8. After the soluble phosphoric acid in ACF-P had been washed out, and most of the residue was metaphosphoric acid or polyphosphates, the  $P_{2p}$  of ACF-P shifted down from 134.2 to 133.7 eV.

The residual metaphosphoric acid or polyphosphates can enhance the adsorption ability of ACF-P for silver ions. The saturation adsorption capacity of ACF-P can reach 150–230 mg/g.

#### FTIR analysis

Figure 9 presents the FTIR spectra of various ACF-P-xxx-1. Many similar rules as obtained from the carbonization of ACF-W or other cellulose materials, as reported in the literatures,<sup>8</sup> can be confirmed.

1. When the activation temperature rose to 250°C, sisal fiber was dehydrated and a conjugated carbonyl group and olefinic bond were produced. The appearance of a peak at  $1700\text{ cm}^{-1}$  for ACF-P-250<sup>-1</sup> shows the formation of the carbonyl group. The strong peak at  $989\text{ cm}^{-1}$ , shown in

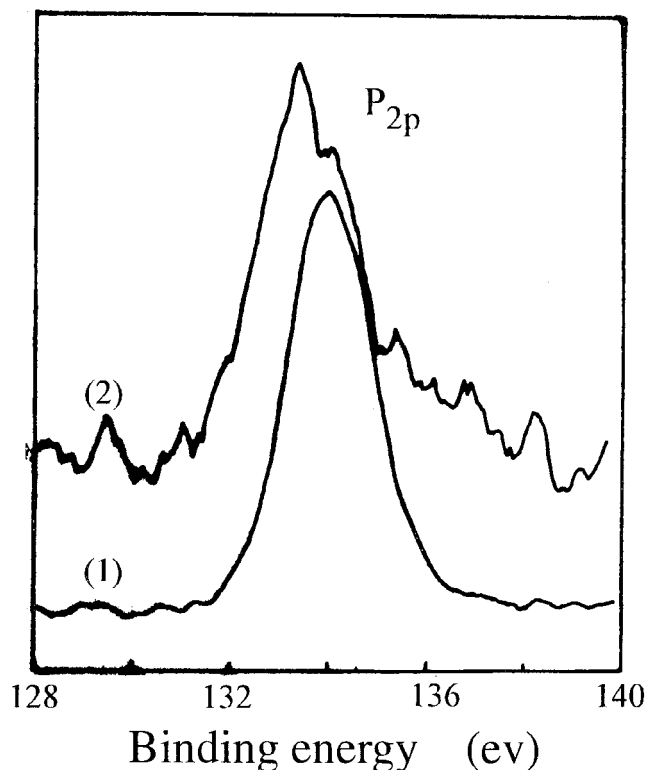
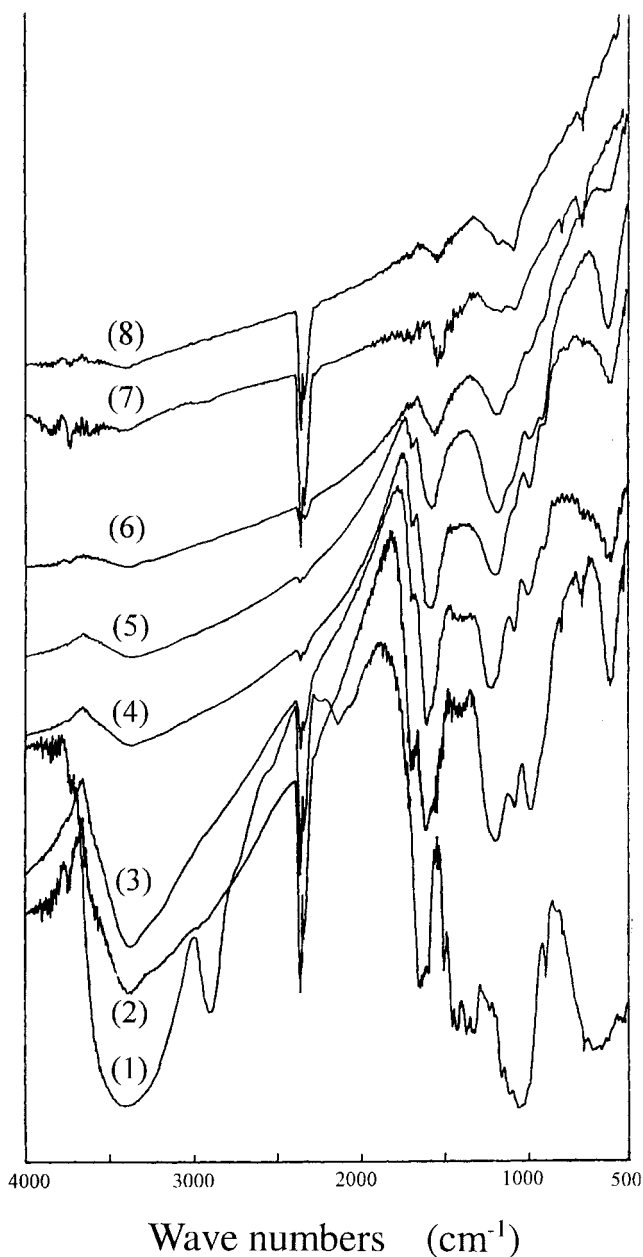


Figure 8 XPS  $P_{2p}$  spectrum of ACF-P-300: (1) ACF-P-300-0, (2) ACF-P-300-1.



**Figure 9** FTIR spectra of ACF-P-xxx-1 activated at different temperatures: (1) 30°C, (2) 250°C, (3) 300°C, (4) 350°C, (5) 400°C, (6) 500°C, (7) 750°C, (8) 830°C.

Figure 9, can be assigned to the strong conjugation of the carbonyl group with olefinic bond.

2. When the activation temperature was greater than 300°C, both peaks at 1700  $\text{cm}^{-1}$  and 989

$\text{cm}^{-1}$  decreased, that is, the amount of carbonyl group and conjugation action decreased.

3. All ACF-Ps had certain amounts of a phenol group (hydroxyl), judging from the remarkable peak at 1000–1200  $\text{cm}^{-1}$ .
4. The intensities of all peaks for ACF-P corresponding with the number of surface groups decreased with the increase of activation temperature. This tendency is the same as that for carbonization of ACF-W.<sup>21</sup> In addition, as observed in  $^{31}\text{P}$ -NMR and  $\text{P}_{2\text{p}}$ -XPS, the peak at 1620  $\text{cm}^{-1}$ , corresponding to the aromatic structure, shifted forward to lower wave numbers (Table VII).

### CONCLUSIONS

The ACF-P activated at low temperature mainly contained graphitelike aromatic carbon structure, as expected, and a certain amount of phenol groups and also acetal (or methylenedioxy) carbon. There were very few methyl, methylene, and carbonyl groups in all the ACF-P activated at different temperatures. The oxygen-containing groups including phenol and acetal groups were greatly reduced at high activation temperature. The formation of graphitelike aromatic structure is thought to play a role in the enhancement of adsorption ability of ACF-P.

Different from the ACF-W, two forms of phosphorus, that is, metaphosphoric acid (or polyphosphates) and elemental phosphorus, were produced on ACF-P. When the ACF-P were activated at low temperature, a lot of phosphoric acid remained in the pores so that the product had to be washed with water to obtain a large surface area. However, when the activation was carried out at high temperature, the washing process could be omitted because most phosphorus compounds had volatilized from the fiber, and unobstructed micropores remained.

As expected, the ACF-P activated at lower temperature possessed a large amount of phenol and other oxygen-containing surface groups and thus had enhanced adsorption ability for polar adsorbates such as methanol. The residual metaphosphoric acid is thought to enhance the adsorption ability of ACF-P for silver ions.

It was discovered that the peaks of  $^{31}\text{P}$ -NMR,  $\text{P}_{2\text{p}}$ -XPS, and FTIR at 1620  $\text{cm}^{-1}$  shift with the increase of an activated temperature, but the detailed shift mechanism is unclear at present.

**TABLE VII**  
Shift of Aromatic IR Peak of ACF-P-xxx-1

Activation temperature (°C)	250	300	350	400	500	830
Peak's wavenumbers ( $\text{cm}^{-1}$ )	1617.3	1613.6	1585.4	1575.2	1564.5	1540.6



## References

1. Zeng, H.; Fu, R. *J Funct Mater (China)* 1991, 22(6), 321.
2. Macnair, R. N.; Arons, G. N. In *Carbon Adsorption Handbook*; Cheremisinoff, P. N., Ellerbusch, F., Eds.; Science Publishers: Ann Arbor, MI, 1978; pp 810–859.
3. Ishizaki, N. *Chemical Engineering (Japan)* 1984, 29(7), 24.
4. Fu, R.; Liu, L.; Lu, Y.; Yue, Z.; Zeng, H. *Ion Exchange and Adsorption (China)*, 1998, 14(5), 411.
5. Fu, R.; Liu, L.; Lu, Y.; Zeng, H. *New Carbon Materials (China)*, 1997, 12(4), 39.
6. Fu, R.; Zhang, Y.; Fang, M.; Zeng, H. *Chinese J Mat Res (China)* 2000, 14(4), 367.
7. Fu, R.; Liu, L.; Zeng, H. *J Appl Polym Sci*, to appear.
8. Tang, M. M.; Bacon, R. *Carbon* 1964, 2, 211.
9. Mangun, C. L.; Benak, K. R.; Daley, M. A. *J Economy, Chemistry of Materials*, 1999, 11(12), 3476.
10. Shin, S.; Jang, J.; Yoon, S. H.; Mochida, I. *Carbon* 1997, 35, 12, 1739.
11. Elmerraoui, M.; Aoshima, M.; Kaneko, K. *Langmuir* 2000, 16(9), 4300.
12. Elmerraoui, M.; Tamai, H.; Yasuda, H.; Kanata, T.; Mondori, J.; Nadai, K.; Kaneko, K. *Carbon* 1998, 36(12), 1769.
13. Biniak, S.; Szymanski, G.; Siedlewski, J.; Swiatkowski, A. *Carbon* 1997, 35(12), 1799.
14. Takabagi, T.; Ishitani, A. *Carbon* 1988, 26(3), 389.
15. Kozlowski, C.; Sherwood, P. M. A. *Carbon* 1987, 25(6), 751; 1986, 24(3), 357.
16. Azami, K.; Yamamoto, S.; Yokono, T.; Sanada, Y. *Carbon* 1991, 29(7), 943.
17. Azami, K.; Yamamoto, S.; Sanada, Y. *Carbon* 1993, 31(4), 611.
18. Frigge, K.; Buechtemann, A.; Fink, H. P. *Acta Polym* 1991, 42(7), 322.
19. Luking, P. B.; McKenzie, D. R.; Vassallo, A. M.; Hanna, J. V. *Carbon* 1993, 31(4), 569.
20. Fu, R.; Zeng, H. *Synthetic Fiber Industry* 1990, 13(5), 19.
21. Fu, R.; Zeng, H.; Lu, Y.; Lai, S. Y.; Chan, W. H.; Ng, C. F. *Ion Exchange and Adsorption*, 1998, 14(5), 419.
22. Fu, R.; Liu, L.; Zeng, H.; Huang, W.; Sun, P. *Chinese J Reactive Polym* 1999, 8(1–2), 12.
23. Jagtoyen, M.; Thwaites, M.; Stencil, J.; McEnaney, B.; Derbyshire, F. *Carbon*, 1992, 30(7), 1089.
24. Toles, C.; Rimmer, S.; Hower, J. C. *Carbon* 1996, 34, 1419.
25. Benaddi, H.; Bandosz, T. J.; Jagiello, J.; Schwarz, J. A.; Rouzaud, J. N.; Legras, D.; Beguin, F. *Carbon* 2000, 38(5), 669.
26. Girgis, B. S.; Ishak, M. F. *Mater Lett* 1999, 39(2), 107.
27. Diao, Y. L.; Walawender, W. P.; Fan, L. T. *Advances in Environmental Research* 1999, 3(3), 333.
28. Zhang, M.; Zhu, S.; Zeng, H.; Lu, Y. *Die Angewandte Makromolekulare Chemie* 1994, 222, 147.
29. Azami, K.; Yamamoto, S.; Yokono, T.; Sanada, Y. *Carbon* 1991, 29(7), 943.
30. Azami, K.; Yamamoto, S.; Sanada, Y. *Carbon* 1993, 31(4), 611.
31. Frigge, K.; Buechtemann, A.; Fink, H. P. *Acta Polym* 1991, 42(7), 322.
32. Dean, J. A. *Lange's Handbook of Chemistry*, 13th ed.; McGraw-Hill: New York, 1985.
33. Stothers, J. B. *<sup>13</sup>C-NMR Spectroscopy*; Academic Press, London 1972.
34. Fu, R.; Zeng, H. *Synthetic Fiber Industry (China)* 1990, 13(5), 19.
35. Wagner, C. D.; Riggs, W. M.; Davis, L. E.; Moulder, J. F.; Muilenberg, G. E. *Handbook of X-ray Photoelectron Spectroscopy*; Perkin-Elmer Corporation, Physical Electronic Division, Eden Prairie, MN, 1978.